Supporting Information for

Covalent organic framework constructed from a donor-acceptor-donor motif monomer for photocatalytic hydrogen evolution from water

Guang-Bo Wang,†[a] Hai-Peng Xu,†[a] Ke-Hui Xie,[a] Jing-Lan Kan,[a] Jianzhong Fan,[b] Yan-Jing Wang,[a] Yan Geng [a]* and Yu-Bin Dong [a]*

[a] College of Chemistry, Chemical Engineering and Materials Science, Collaborative Innovation Center of Functionalized Probes for Chemical Imaging in Universities of Shandong, Key Laboratory of Molecular and Nano Probes, Ministry of Education, Shandong Normal University, Jinan 250014, P. R. China. E-mail: gengyan@sdnu.edu.cn; yubindong@sdnu.edu.cn.

[b] School of Physics and Electronics, Shandong Normal University, Jinan 250014, P. R. China.

† These authors contributed equally to this work.

General methods

^{1}H and ^{13}C NMR were recorded on a Bruker Avance 400 NMR spectrometer. Powder X-ray diffraction (PXRD) data were collected using a SmartLab SE X-ray powder diffractometer (Rigaku, Japan) with Cu K_{α} radiation (λ = 1.5405 Å) in the range of 2θ = 2.00°-30.00° at a step size of 0.1°. Fourier Transform Infrared (FT-IR) spectra in the region of 500-4000 cm^{-1} were obtained with a Perkin-Elmer 1600 FT-IR spectrometer. Thermogravimetric analysis (TGA) was performed on a Mettler Toledo TGA/DSC3+ thermogravimetric analyzer in the temperature range of 20-800 ºC under an N_2 atmosphere and a heating rate of 10 °C/min. The scanning electron microscopy (SEM) images of the **DABT-Py-COF** material were recorded on a Hitachi SU8010 scanning electron microscope with acceleration voltage of 20 kV and the high-resolution transmission electron microscopy (HR-TEM) analysis was performed on a JEOL 2100 Electron Microscope with an operating voltage of 200 kV. X-ray photoelectron spectroscopy (XPS) data were obtained with a PHI 5000 Versaprobe II (VP-II) electron spectrometer from Ulvac-Phi. Solid state ^{13}C CP-MAS NMR spectrum was recorded on a Bruker Advance III 400 MHz NMR spectrometer. Solid state ultraviolet-visible (UV-Vis) spectra were recorded on a Shimadzu UV-2700 double-beam UV-vis spectrophotometer. High-resolution mass spectrometry (HRMS) analysis was detected by Bruker maXis ultrahigh-resolution-TOF mass spectrometer. Time-resolved photoluminescence spectroscopy was measured by time-correlated single photon counting (Hamamatsu photonics, Quantaurus-Tau) with laser (710 nm) as the excitation light source. N_2 adsorption measurements were performed using the Micromeritics ASAP 2020 sorption/desorption analyzer at 77 K, the samples were degassed under high vacuum at 120 °C for 8 h before analysis.

Photoelectrochemical measurements

Cyclic voltammetry (CV) measurements were performed on a CHI 660E in a three-electrode electrochemical cell equipped with a salt bridge and a scan rate of 100 mVs^{-1}. The photocurrent measurements were conducted on a workstation in a standard three-electrode system in dark and light excitation at -0.14 V vs. Ag/AgCl with the photocatalyst-coated FTO as the working electrode, Pt plate as the counter electrode and Ag/AgCl as the reference electrode by directly irradiating the working electrode from the back side using a 300 W Xenon lamp with AM 1.5 cut-off filter, and 2M Na_2SO_4 aqueous solution was used as the electrolyte. Electrochemical impedance spectroscopy (EIS) analysis was performed at the open circuit condition at -0.14 V vs. Ag/AgCl in the frequency range of 0.01 to 10000 Hz with an AC amplitude of 10 mV.

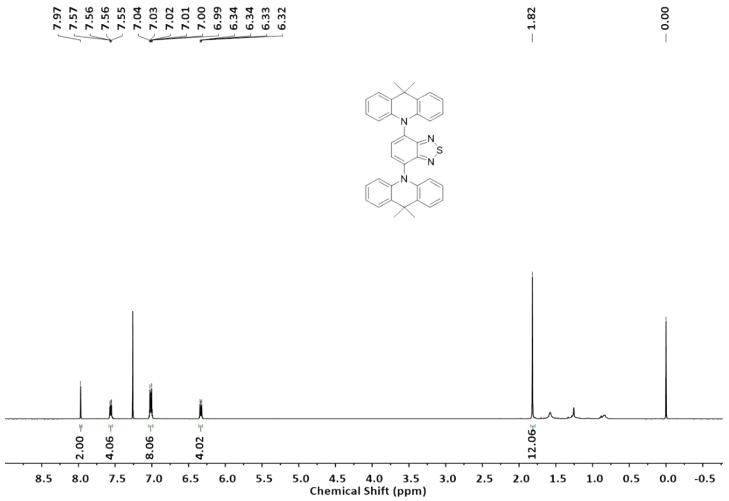

Fig. S1 ^{1}H NMR spectrum of compound **DABT**.

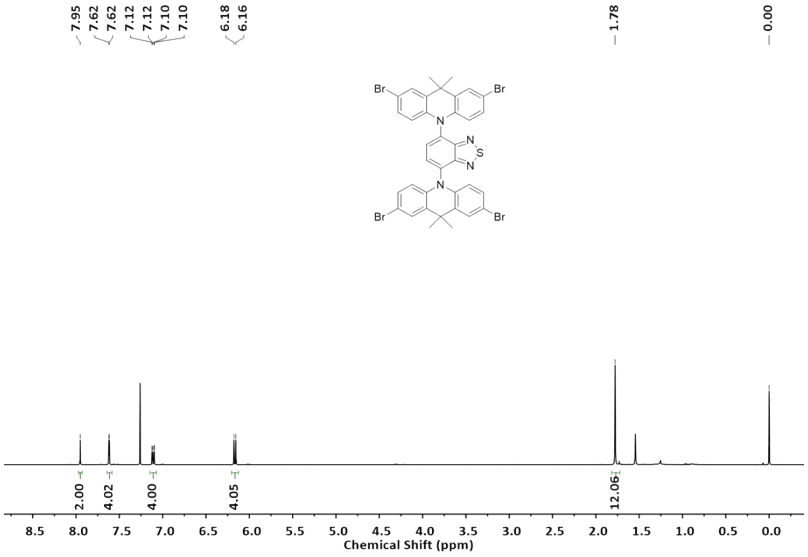

Fig. S2 ^{1}H NMR spectrum of compound **DABT-4Br**.

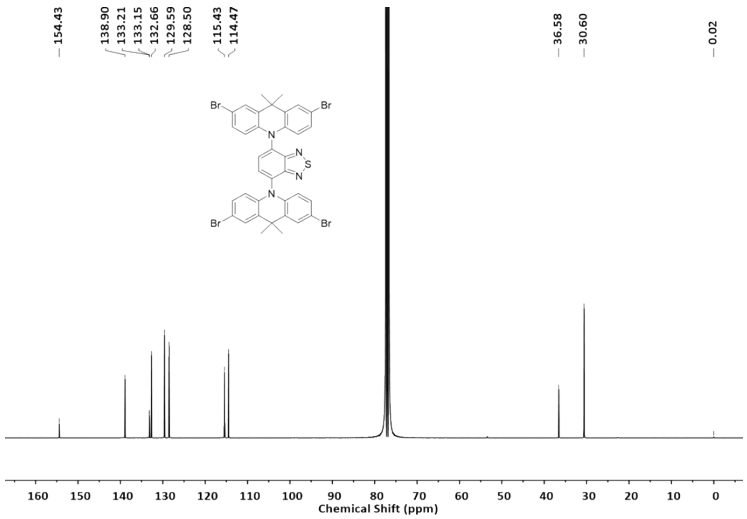

Fig. S3 ^{13}C NMR spectrum of compound **DABT-4Br**.

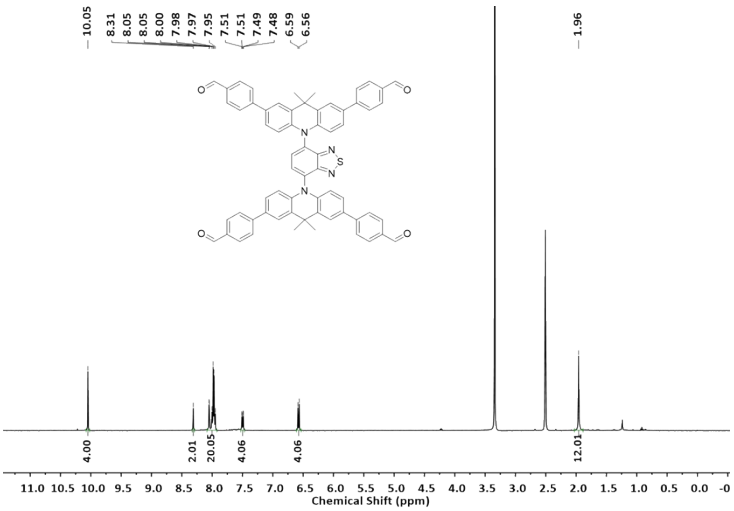

Fig. S4 ^{1}H NMR spectrum of **DABT-4CHO**.

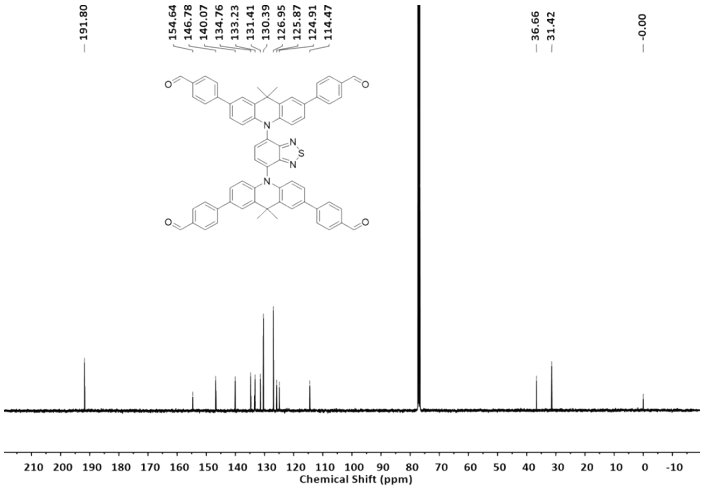

Fig. S5 ^{13}C NMR spectrum of **DABT-4CHO**.

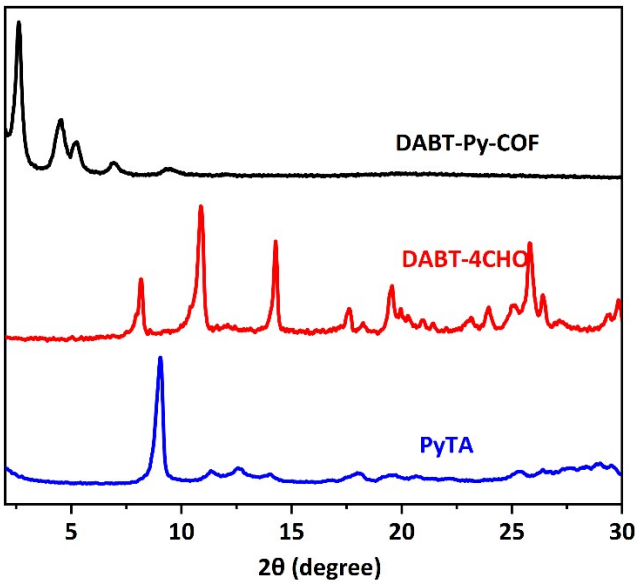

Fig. S6 Comparison of the PXRD patterns of the PyTA (blue), **DABT-4CHO** (red) and the DABT-Py-COF (black).

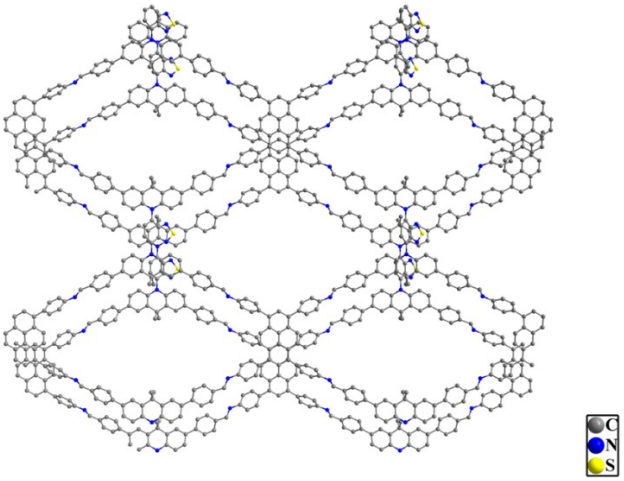

Fig. S7 Top view of the ball-stick model of **DABT-Py-COF** in slipped AA stacking mode.

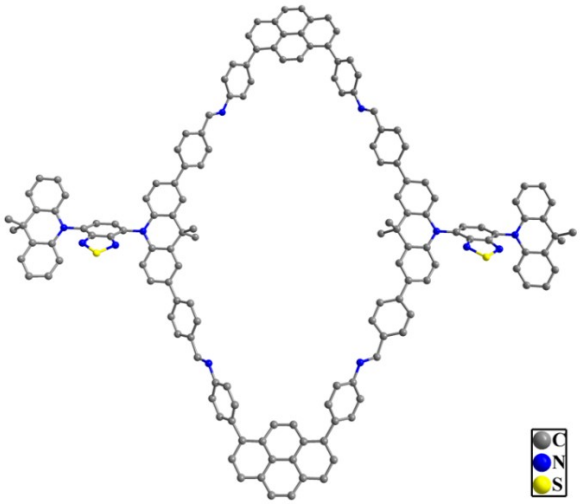

Fig. S8 Ball-stick model of the COF segment.

Table S1 Fractional atomic coordinates for the unit cell of **DABT-Py-COF** with slipped AA stacking.

Space group： *P1* *a* = 33.4252Å, *b* = 28.0981Å, *c* = 7.0436Å *α* = 44.9959°, β = 90.0502°, γ = 90.0440°			
C1	0.51282	2.15798	-6.44277
N2	0.53933	2.11076	-6.25994
S3	0.56721	2.13458	-6.13948
C4	0.45125	3.06441	-6.54015
C5	0.45014	3.00913	-6.5138
C6	0.48957	2.97439	-6.48142
C7	0.41146	2.98326	-6.50574
C8	0.45232	2.3533	-6.67348
C9	0.37819	2.34527	-6.61635
C10	0.41502	2.32202	-6.62533

C11	0.91789	2.74074	-6.65246
C12	0.91806	2.69592	-6.67946
C13	0.95331	2.66461	-6.65577
C14	0.99021	2.68502	-6.62666
C15	0.99004	2.73173	-6.59793
C16	0.95294	2.75738	-6.59817
C17	1.02696	2.75256	-6.5712
C18	1.02787	2.80096	-6.55432
C19	0.98967	2.82232	-6.53961
C20	0.95159	2.80075	-6.55541
C21	1.02728	2.65932	-6.62631
C22	1.06258	2.67801	-6.58305
C23	1.0624	2.72277	-6.55568
C24	0.9523	2.61574	-6.67004
C25	0.99045	2.59299	-6.67765
C26	1.02845	2.61442	-6.6609
C27	0.91067	2.82227	-6.52346
C28	1.06852	2.83061	-6.56246
C29	0.91163	2.58689	-6.66611
C30	1.0692	2.59091	-6.68281
C31	0.90031	2.88999	-6.66977
C32	0.86122	2.90863	-6.65353
C33	0.83027	2.86034	-6.48983
C34	0.84115	2.79296	-6.33889
C35	0.88009	2.77447	-6.35111
C36	1.09727	2.85808	-6.76646
C37	1.13593	2.87988	-6.76748
C38	1.14854	2.87722	-6.56829
C39	1.11954	2.8518	-6.3667
C40	1.08053	2.82951	-6.3652
C41	1.08165	2.52251	-6.49713
C42	1.12074	2.50281	-6.50712
C43	1.14951	2.55072	-6.70558
C44	1.1365	2.61856	-6.89382
C45	1.09773	2.63798	-6.88332
C46	0.88207	2.56124	-6.46848
C47	0.84344	2.54016	-6.47193
C48	0.83165	2.54198	-6.66994
C49	0.86146	2.5655	-6.86479
C50	0.90049	2.58679	-6.86111
N51	0.78825	2.87637	-6.47814
N52	1.18999	2.89949	-6.58039
N53	1.19104	2.53439	-6.7244

N54	0.79024	2.52042	-6.66256
C55	0.77412	2.92962	-6.53609
C56	0.72992	2.94175	-6.50779
C57	0.72251	2.98169	-6.45786
C58	0.68332	3.0001	-6.44971
C59	0.64809	2.98184	-6.49936
C60	0.65527	2.94044	-6.54491
C61	0.69502	2.92068	-6.54775
C62	0.60569	3.00894	-6.51345
C63	0.6026	3.06887	-6.57556
C64	0.56545	3.09732	-6.60249
C65	0.52792	3.0665	-6.55417
C66	0.52913	3.00743	-6.50305
C67	0.56797	2.97935	-6.47987
C68	0.48991	2.97444	-6.70144
C69	1.20694	2.90791	-6.435
N70	1.48959	3.09596	-6.56774
C71	1.48873	2.90109	-6.20102
C72	1.37385	3.00786	-6.50822
C73	1.48951	3.15531	-6.60319
C74	1.46702	3.21495	-6.80709
C75	1.33191	2.97953	-6.48991
C76	1.30036	2.97278	-6.3376
C77	1.26136	2.94985	-6.32411
C78	1.25048	2.93286	-6.46498
C79	1.28184	2.93916	-6.61814
C80	1.32152	2.9613	-6.62821
C81	0.77338	2.51406	-6.81463
C82	1.20873	2.4749	-6.57687
C83	0.51345	2.21317	-6.4756
C84	0.48998	2.27157	-6.66751
N85	0.54073	2.20647	-6.31886
N86	0.49021	2.32958	-6.69497
C87	0.52844	2.36254	-6.73116
C88	0.53019	2.4117	-6.72234
C89	0.49106	2.44115	-6.71942
C90	0.5652	2.34779	-6.78183
C91	0.60256	2.37378	-6.79313
C92	0.60618	2.41787	-6.76108
C93	0.56907	2.43681	-6.72951
C94	0.48944	2.51659	-6.9856
C95	0.64829	2.4449	-6.77319
C96	0.67924	2.45663	-6.94015

C97	0.71829	2.47868	-6.94905
C98	0.72979	2.49007	-6.78993
C99	0.69905	2.47897	-6.62265
C100	0.65936	2.45746	-6.61603
C101	1.45143	2.40786	-6.69526
C102	1.4129	2.43182	-6.69113
C103	1.37543	2.40122	-6.65153
C104	1.49368	2.43382	-6.48019
C105	1.33366	2.42369	-6.63481
C106	1.32206	2.49185	-6.7941
C107	1.28239	2.51017	-6.78269
C108	1.25229	2.46117	-6.60835
C109	1.26443	2.3936	-6.44718
C110	1.3034	2.37556	-6.4603
C111	1.46672	3.27087	-6.83534
C112	0.41366	3.08628	-6.53014
H113	0.41052	2.94181	-6.48801
H114	0.35125	2.31894	-6.58414
H115	0.41359	2.27802	-6.59074
H116	0.88953	2.76356	-6.6818
H117	0.88979	2.68731	-6.72573
H118	0.98957	2.85665	-6.5171
H119	1.09119	2.65716	-6.56478
H120	1.09087	2.73262	-6.51617
H121	0.9906	2.55778	-6.69558
H122	0.92217	2.9293	-6.80446
H123	0.85503	2.96129	-6.77613
H124	0.81904	2.75369	-6.20913
H125	0.88594	2.72184	-6.22873
H126	1.09002	2.86164	-6.926
H127	1.15649	2.899	-6.92717
H128	1.12693	2.84786	-6.20657
H129	1.06012	2.80929	-6.20342
H130	1.06139	2.48389	-6.33812
H131	1.12827	2.44991	-6.35601
H132	1.15683	2.65752	-7.05104
H133	1.09019	2.69087	-7.03205
H134	0.88867	2.55846	-6.31041
H135	0.82224	2.52238	-6.31704
H136	0.85475	2.56858	-7.02331
H137	0.92158	2.60549	-7.01787
H138	0.79558	2.96654	-6.59076
H139	0.74766	2.99931	-6.42415

H140	0.68108	3.02936	-6.40337
H141	0.6302	2.9245	-6.5861
H142	0.69837	2.8907	-6.59051
H143	0.62915	3.09743	-6.62172
H144	0.56673	3.14637	-6.67519
H145	0.56882	2.93409	-6.43695
H146	0.51854	2.95563	-6.70752
H147	0.48487	3.02623	-6.90147
H148	0.46611	2.9417	-6.66851
H149	1.18872	2.89865	-6.28469
H150	1.48926	2.90069	-6.04199
H151	1.5147	2.87165	-6.17016
H152	1.46147	2.87397	-6.17209
C153	1.37658	3.05933	-6.51612
H154	1.44937	3.21844	-6.9455
H155	1.30584	2.98468	-6.22344
H156	1.23915	2.94571	-6.20111
H157	1.27587	2.92668	-6.72985
H158	1.34396	2.96545	-6.75
H159	0.79157	2.52518	-6.96907
H160	1.19132	2.43047	-6.4192
H161	0.56554	2.31532	-6.8133
H162	0.62913	2.35789	-6.82361
H163	0.57045	2.47335	-6.71913
H164	0.46392	2.54254	-6.98972
H165	0.48636	2.52229	-7.1581
H166	0.51696	2.54356	-7.0166
H167	0.67325	2.44947	-7.06957
H168	0.74003	2.48668	-7.08339
H169	0.70556	2.48698	-6.49644
H170	0.63747	2.44931	-6.48228
H171	1.41207	2.47379	-6.71197
H172	1.5162	2.46853	-6.51615
H173	1.50264	2.38178	-6.29565
H174	1.46496	2.44532	-6.44092
H175	1.34347	2.53159	-6.93305
H176	1.2754	2.56287	-6.91095
H177	1.24326	2.35341	-6.30743
H178	1.30986	2.32254	-6.32815
H179	1.44827	3.31398	-6.99083
H180	1.34947	1.08	0.48601
H181	1.41221	1.12439	0.4712

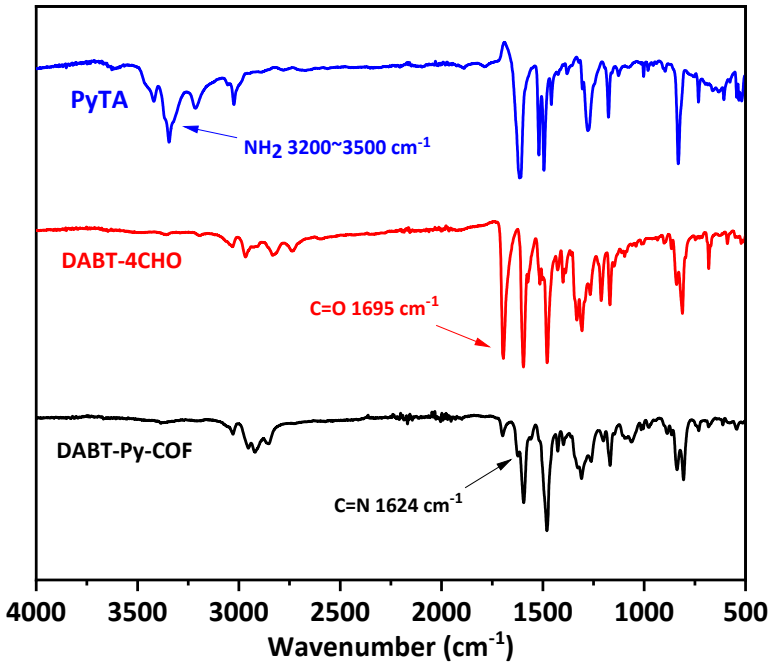

Fig. S9 FT-IR spectra comparison of the PyTA (blue), **DABT-4CHO** (red) and **DABT-Py-COF** (black).

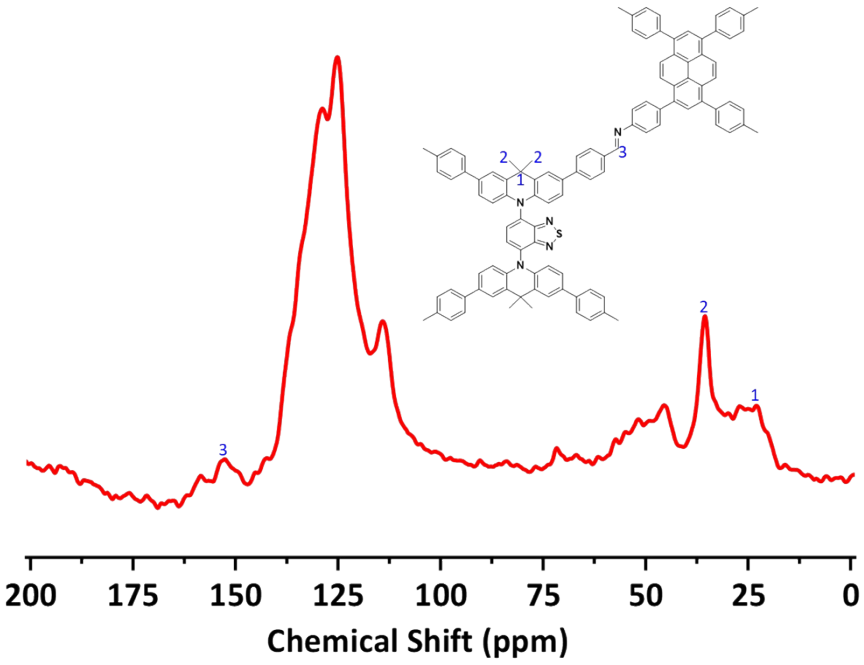

Fig. S10 The solid state ^{13}C cross polarization magic angle spinning (^{13}C CP/MAS) NMR spectrum of **DABT-Py-COF**.

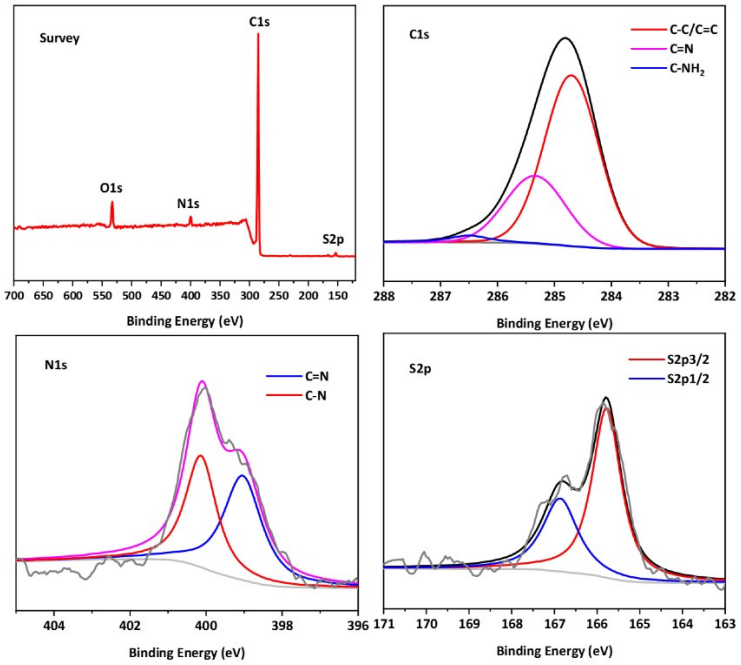

Fig. S11 The X-ray photoelectron spectroscopy (XPS) of the **DABT-Py-COF**, including the survey, C1s, N1s and S2p spectra.

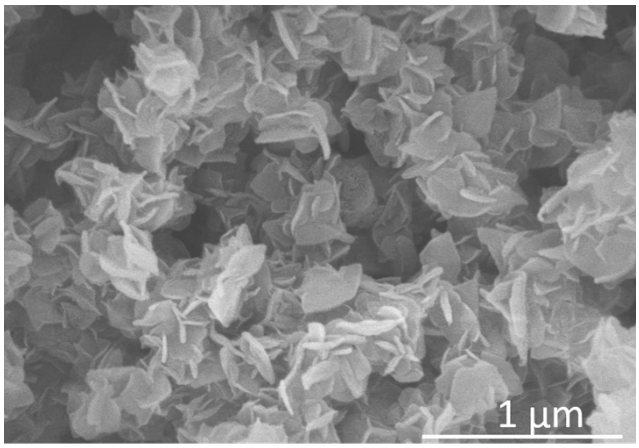

Fig. S12 Scanning electron microscopy (SEM) image of the **DABT-Py-COF**.

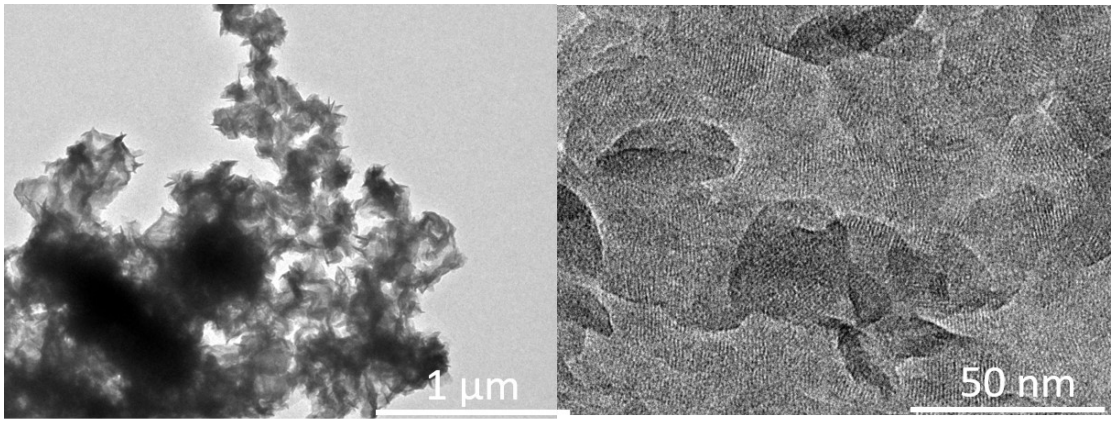

Fig. S13 Transmission electron microscopy (TEM) image of the **DABT-Py-COF**.

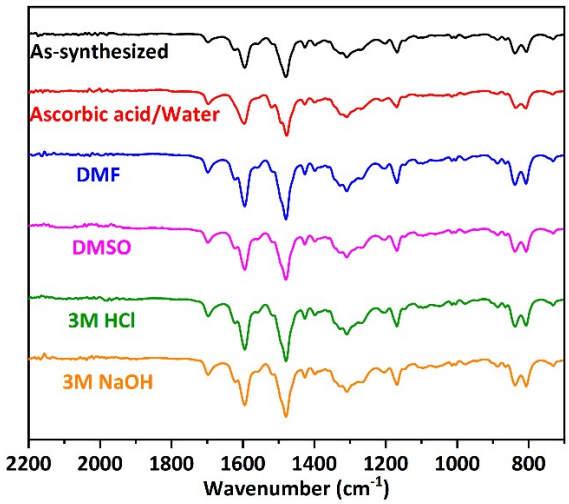

Fig. S14 FT-IR spectra of **DABT-Py-COF** after immersing in different solvents for 1 week.

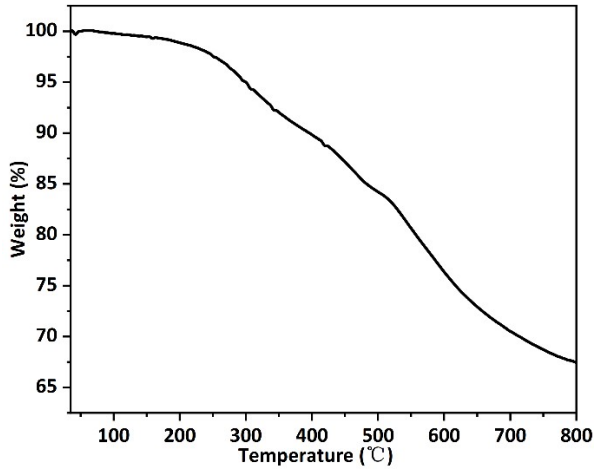

Fig. S15 Thermogravimetric analysis (TGA) curve of the **DABT-Py-COF** measured at a heating rate of 10 ^{o} C/min under a nitrogen flow.

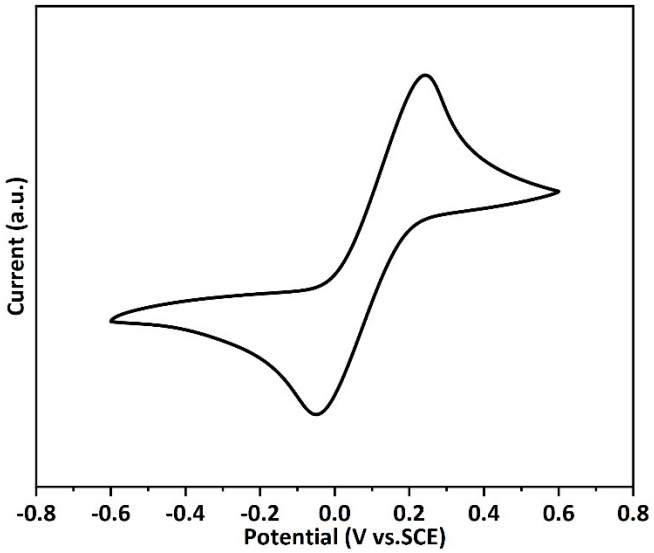

Fig. S16 Cyclic voltammetry measurements of ferrocene/ferrocenium couple to calibrate the pseudo reference electrode ($E_{1/2}$ is obtained to be 0.11 V).

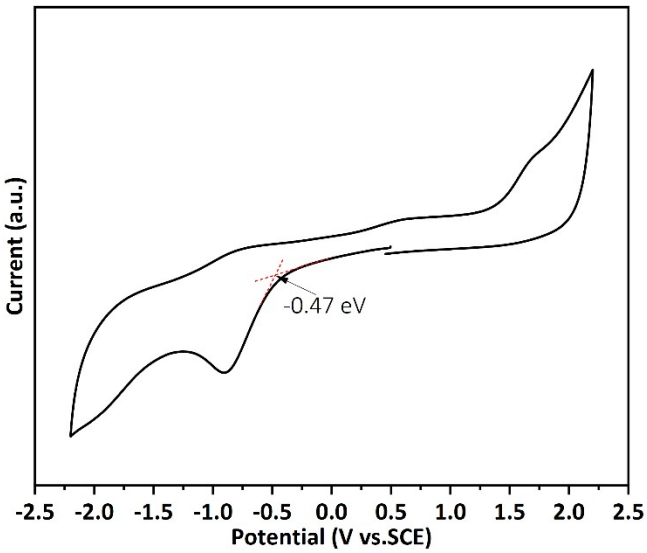

Figure S17. Cyclic voltammetry plot of **DABT-Py-COF** referenced to saturated calomel (SCE) using ferrocene (F_c) as an internal standard at a scan rate of 100 mV S^{-1}. The calculation of the E_{HOMO} and E_{LUMO} is according to the following equations:

$$E_{LUMO} = - (E_{onset\ vs.SCE} - E_{(1/2,Fc)} + 4.8)\ eV$$

$$E_{HOMO} = E_{LUMO} - E_{g,opt}$$

Where, $E_{1/2,\ Fc}$ is obtained to be 0.11 vs. SCE., reduction onset potential $E_{onset\ vs.\ SCE}$ was extracted from the X-intercept of the linear fit in the voltammogram, $E_{g,opt}$ is obtained from the UV-Vis spectrum by using Tauc-plot method.

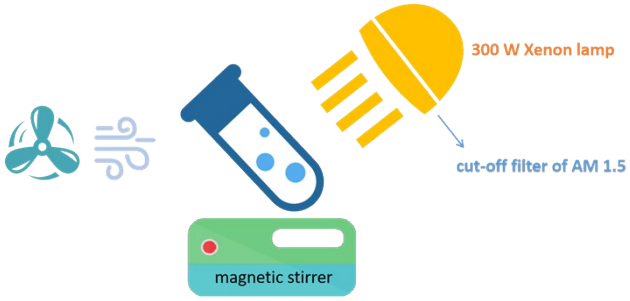

Figure S18. A schematic representation for this photocatalytic H2 evolution.

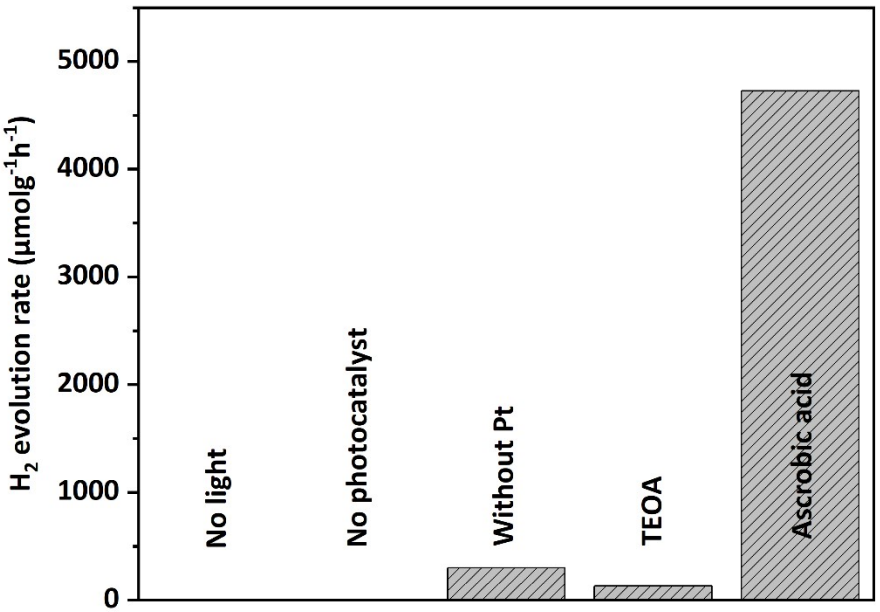

Fig. S19 Photocatalytic performance of **DABT-Py-COF** over 4h under visible-light irradiation (AM 1.5) in the absence of light/ photocatalyst/Pt co-catalyst and in the presence of sacrificial agent of TEOA or ascorbic acid.

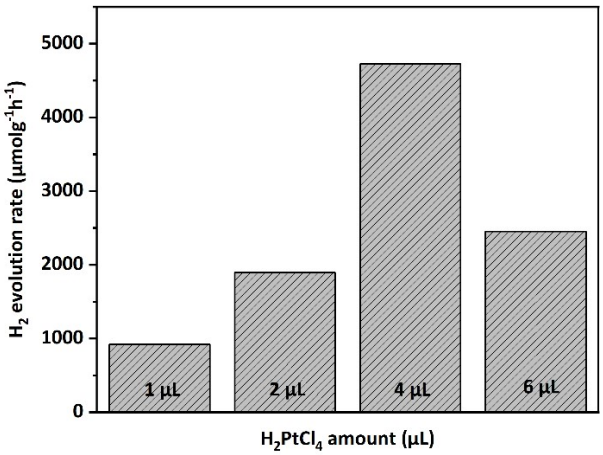

Fig. S20 The effects of the Pt amount on the photocatalytic performance of the **DABT-Py-COF**.

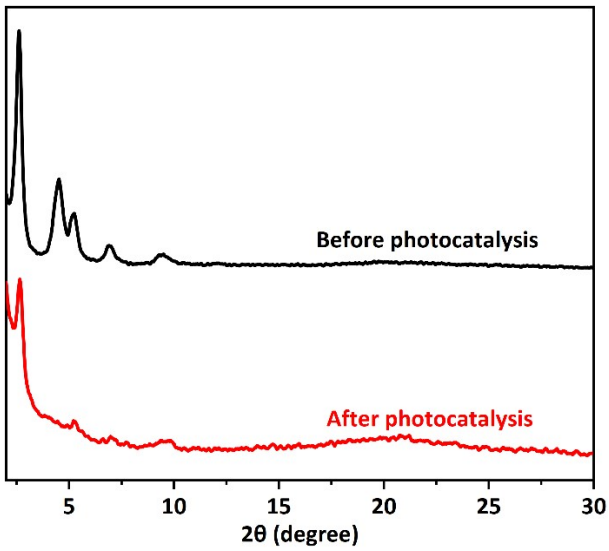

Fig. S21 PXRD patterns of the **DABT-Py-COF** before and after 5 cycles photocatalytic reactions.

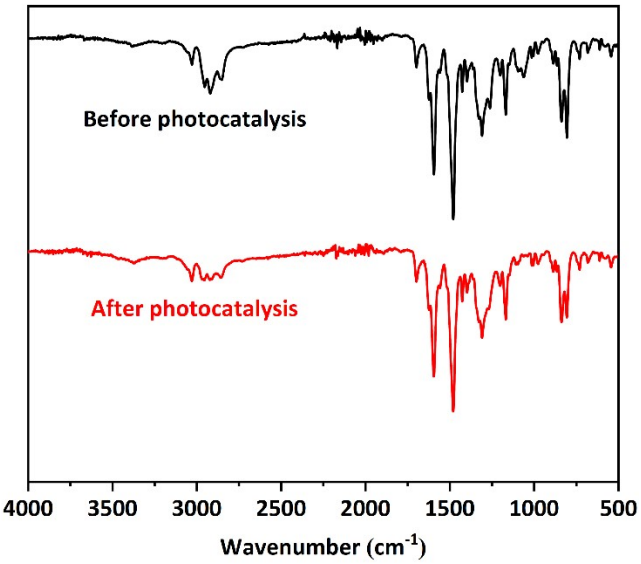

Fig. S22 FT-IR spectra of the **DABT-Py-COF** before and after 5 cycles photocatalytic reactions.

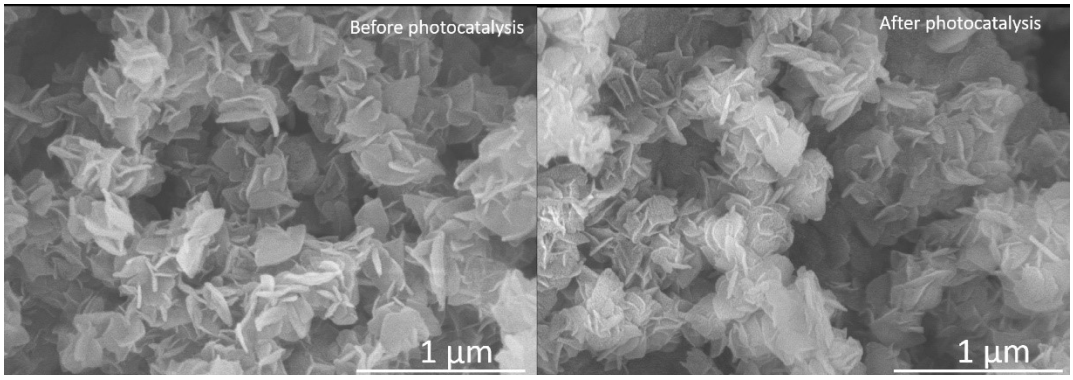

Fig. S23 Scanning electron microscopy (SEM) images of the **DABT-Py-COF** before and after 5 cycles photocatalytic reactions.

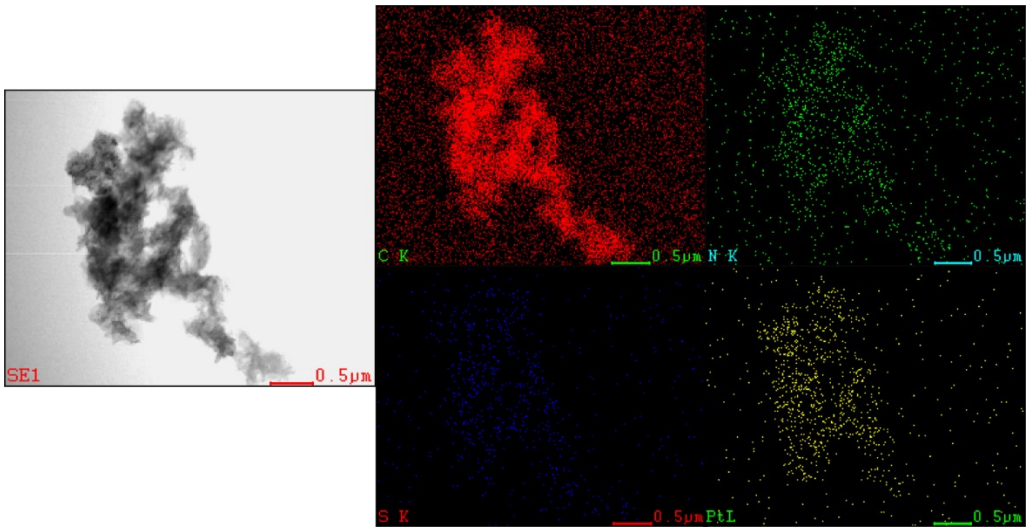

Fig. S24 Transmission electron microscopy (TEM) and EDS mapping of the **DABT-Py-COF** after photocatalytic reactions.

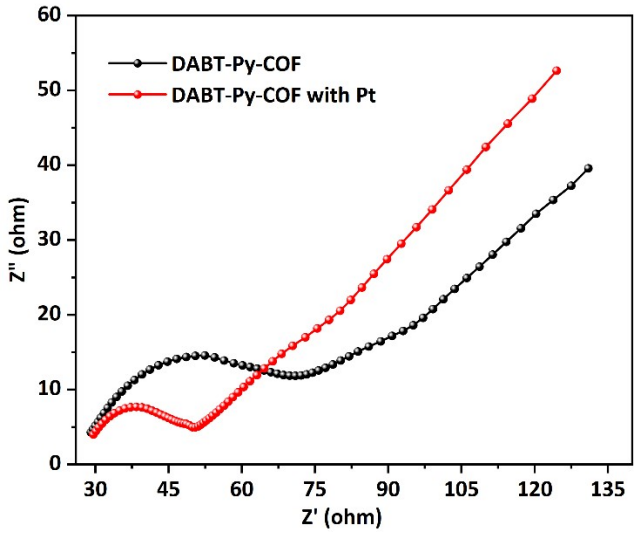

Fig. S25 Electrochemical impedance spectroscopy (EIS) Nyquist plots of the **DABT-Py-COF** with and without the Pt co-catalyst.

Table S2. The summary of the photocatalytic H_2 evolution performance under visible-light irradiation over different types of CMPs and COFs.

COFs	Band gap (eV)	Co-catalyst	Sacrificial agent	HER (μmol g^{-1} h^{-1})	Ref.
g-$C_{40}N_3$-COF	2.36	Pt	Na_2S	4	2
TPAL-COF	-	Pt	TEOA	6.8	3
g-$C_{40}N_3$-COF	2.36	Pt	TEA	12	2
g-$C_{40}N_3$-COF	2.36	Pt	Na_2SO_3	14	2
N_0-COF	2.6-2.7	Pt	TEOA	23	4
TpPa-2-COF	2.52	Pt	Lactic acid	28	5
g-$C_{40}N_3$-COF	2.36	Pt	EtOH	56	2
TpPa-2	2.07	Pt	Sodium	72.09	6

			ascorbate		
BE-COF	2.12	Pt	Ascorbic acid	76.0	7
PTP-COF	2.1	Pt	TEOA	83.83	8
N_1-COF	2.6-2.7	Pt	TEOA	90	6
N_1-COF	-	Co-1	TEOA	100	9
CTP-1	2.96	Pt	TEOA	120	10
sp^2 c-CMP	1.96	Pt	TEOA	140	11
TTR-COF	2.71	Au	TEOA	141	12
TTB-COF	2.8	Au	TEOA	145.25	12
N3-COF	-	Co-1	TEOA	163	9
OB-POP-1	2.21	Pt	TEOA	168	13
CTF-1	2.23	Pt	TEOA	168	14
B-CTF-1	2.14	Pt	TEOA	179	14
TpPa-COF-NO_2	1.92	Pt	Sodium ascorbate	220	15
COF-42	-	Co-1	TEOA	233	9
TP-BDDA	2.31	Pt	TEOA	324 ± 10	16
CTF-15	2.58	Pt	TEA	352	17
TBC-COF	-	Pt	TEOA	360	14
N_2-COF	-	Co-2[b]	TEOA	414	9
N_2-COF	2.6-2.7	Pt	TEOA	438	4
CTP_{300}	2.36	Pt	TEOA	500	10
TAB-TFP-COF	2.45	Pt	Ascorbic acid	666.4	18
N_2-COF	-	Co-1[a]	TEOA	782	9
OB-POP-2	2.28	Pt	TEOA	940	13
TpDTz COF	2.07	NiME	TEOA	941	19
CTF-1-10min	2.26	Pt	TEOA	1072	20
CTF-Th	2.38	Pt	TEOA	1100	21
OB-POP-4	2.37	Pt	TEOA	1114	13
TpPa-1-COF	2.02	Pt	Sodium ascorbate	1223	22
OB-POP-3	2.14	Pt	TEOA	1322	13
sp^2 c-COF	1.9	Pt	TEOA	1360	11
CTF-O	2.67	Pt	TEOA	1440	23
CTF-HUST-1	2.03	Pt	TEOA	1540	24
TpPa-COF	2.09	Pt	Sodium ascorbate	1560	15
TP-COF	2.28	Pt	Ascorbic acid	1600 (±80)	25
N_3-COF	2.6-2.7	Pt	TEOA	1703	4
CTF-BT	2.51	Pt	TEOA	1800	21
$Ni(OH)_2$-2.5%/TpPa-2	-	$Ni(OH)_2$	Sodium ascorbate	1895.99	6
TFPT-COF	2.8	Pt	TEOA	1970	26
$CTFS_{10}$	1.87	Pt	TEOA	2000	27

sp^2 c-COF_{ERDN}	1.85	Pt	TEOA	2120	11
COF-alkene	2.34	Pt	TEOA	2330	28
g-$C_{40}N_3$-COF	2.36	Pt	TEOA	2596	2
Py-FTP-BTCOF	2.34	Pt	Ascorbic acid	2875	29
TpPa-COF-CH_3	2.10	Pt	Sodium ascorbate	3070	15
CdS-COF(90:10)	-	Pt	Lactic acid	3678	5
TZ-COF-4	2.2	Pt	Ascorbic acid	4296	30
S-COF	2.10	Pt	Ascorbic acid	4440 (±140)	25
PyTA-BC	2.71	Pt	Ascorbic acid	5030	31
CTF-S	2.47	Pt	TEOA	5320	23
TpPa-1	2.11	Pt	Ascorbic acid	5479	32
MoS2-3%/TpPa-1-COF	2.14	MoS_2	Ascorbic acid	5585	32
CTF-$HS_{0.75}$-1	2.70	Pt	TEOA	6040	24
CTF-BT/Th-1	2.51	Pt	TEOA	6606	21
CTF-$HS_{0.75}$-2	-	Pt	TEOA	7100	24
TpPa-COF-$(CH_3)_2$	2.06	Pt	Sodium ascorbate	8330	15
TP-COF	1.97	PVP-Pt	Ascorbic acid	8420	7
CTF-CBZ	2.17	Pt	TEOA	9920	33
CN-COF	2.09	Pt	TEOA	10100	34
Pd^0/TpPa-1-EosinY	-	-	TEOA	10400	35
CTF-N	2.17	Pt	TEOA	10760	33
20%CdS-CTF-1	-	Pt	Lactic acid	11430	36
CdS NPs/3%CTF-1	2.36	Pt	Lactic acid	12150	37
Mo_3S_{13}@EB-COF	-	$Ru(bpy)_3Cl_2$	Ascorbic acid	13215	38
ter-CTF-0.7	2.11	Pt	TEOA	19320	33
NH_2-UiO-66/TpPa-1-COF(4:6)	2.10	Pt	Sodium ascorbate	23413	22
FS-COF	1.85	Pt	Ascorbic acid	10100 (±300)	25
NTU−BDA-THTA/NH2−Ti_3C_2Tx(8:4)	2.09	Pt	Ascorbic acid	14228.1	39
BTH-3	-	Pt	Ascorbic acid	15100	40
FS-COF+WS5F	-	Pt	Ascorbic acid	16300 (±290)	25
USTB-10	1.52	Pt	Ascorbic acid	21800	41
WO_3@TpPa-1-COF/rGo (30%)	2.11	Pt	Ascorbic acid	26730	42
COF-JLU100	1.4	Pt	TEOA	107380	43

Reference

1. F. Ni, Z. Wu, Z. Zhu, T. Chen, K. Wu, C. Zhong, K. An, D. Wei, D. Ma, C. Yang, *J. Mater. Chem. C*, 2017, **5**, 1363-1368.
2. S. Bi, C. Yang, W. Zhang, J. Xu, L. Liu, D. Wu, X. Wang, Y. Han, Q. Liang and F. Zhang, *Nat. Commun.*, 2019, **10**, 2467.
3. R. Lu, C. Liu, Y. Chen, L. Tan, G. Yuan, P. Wang, C. Wang and H. Yan, *J. Photochem. Photobiol.*, A, 2021, **421**, 113546.
4. V. S. Vyas, F. Haase, L. Stegbauer, G. Savasci, F. Podjaski, C. Ochsenfeld and B. V. Lotsch, *Nat. Commun.*, 2015, **6**, 8508.
5. J. Thote, H. B. Aiyappa, A. Deshpande, D. Díaz Díaz, S. Kurungot and R. Banerjee, *Chem. – A Eur. J.*, 2014, **20**, 15961-15965.
6. H. Dong, X.-B. Meng, X. Zhang, H.-L. Tang, J.-W. Liu, J.-H. Wang, J.-Z. Wei, F.-M. Zhang, L.-L. Bai and X.-J. Sun, *Chem. Eng. J.*, 2020, **379**, 122342.
7. J. Ming, A. Liu, J. Zhao, P. Zhang, H. Huang, H. Lin, Z. Xu, X. Zhang, X. Wang, J. Hofkens, M. B. J. Roeffaers and J. Long, *Angew. Chem. int. ed.*, 2019, **131**, 18458-18462.
8. F. Haase, T. Banerjee, G. Savasci, C. Ochsenfeld and B. V. Lotsch, *Faraday Discuss.*, 2017, **201**, 247-264.
9. T. Banerjee, F. Haase, G. Savasci, K. Gottschling, C. Ochsenfeld and B. V. Lotsch, *J. Am. Chem. Soc.*, 2017, **139**, 16228-16234.
10. Z.-A. Lan, Y. Fang, X. Chen and X. Wang, *Chem. Commun.*, 2019, **55**, 7756-7759.
11. E. Jin, Z. Lan, Q. Jiang, K. Geng, G. Li, X. Wang and D. Jiang, *Chem*, 2019, **5**, 1632-1647.
12. L. Li, Z. Zhou, L. Li, Z. Zhuang, J. Bi, J. Chen, Y. Yu and J. Yu, *ACS Sustainable Chem. Eng.*, 2019, **7**, 18574-18581.
13. S. Bi, Z.-A. Lan, S. Paasch, W. Zhang, Y. He, C. Zhang, F. Liu, D. Wu, X. Zhuang, E. Brunner, X. Wang and F. Zhang, *Adv. Funct. Mater.*, 2017, **27**, 1703146.
14. F. Li, D. Wang, Q.-J. Xing, G. Zhou, S.-S. Liu, Y. Li, L.-L. Zheng, P. Ye and J.-P. Zou, *Appl. Catal. B: Environ.*, 2019, **243**, 621-628.
15. J.-L. Sheng, H. Dong, X.-B. Meng, H.-L. Tang, Y.-H. Yao, D.-Q. Liu, L.-L. Bai, F.-M. Zhang, J.-Z. Wei and X.-J. Sun, *ChemCatChem*, 2019, **11**, 2313-2319.
16. P. Pachfule, A. Acharjya, J. Roeser, T. Langenhahn, M. Schwarze, R. Schomäcker, A. Thomas and J. Schmidt, *J. Am. Chem. Soc.*, 2018, **140**, 1423-1427.
17. C. B. Meier, R. Clowes, E. Berardo, K. E. Jelfs, M. A. Zwijnenburg, R. S. Sprick and A. I. Cooper, *Chem. Mater.*, 2019, **31**, 8830-8838.
18. X. Wu, M. Zhang, Y. Xia, C. Ru, P. Chen, H. Zhao, L. Zhou, C. Gong, J. Wu, X. Pan, *J. Mater. Chem. A*., 2022, **10**, 17691.
19. B. P. Biswal, H. A. Vignolo-González, T. Banerjee, L. Grunenberg, G. Savasci, K. Gottschling, J. Nuss, C. Ochsenfeld and B. V. Lotsch, *J. Am. Chem. Soc.*, 2019, **141**, 11082-11092.
20. S. Kuecken, A. Acharjya, L. Zhi, M. Schwarze, R. Schomäcker and A. Thomas, *Chem. Commun.*, 2017, **53**, 5854-5857.
21. W. Huang, Q. He, Y. Hu and Y. Li, *Angew. Chem.*, 2019, **131**, 8768-8772.
22. F.-M. Zhang, J.-L. Sheng, Z.-D. Yang, X.-J. Sun, H.-L. Tang, M. Lu, H. Dong, F.-C. Shen, J. Liu and Y.-Q. Lan, *Angew. Chem.*, 2018, **130**, 12282-12286.

23. L. Guo, Y. Niu, H. Xu, Q. Li, S. Razzaque, Q. Huang, S. Jin and B. Tan, *J. Mater. Chem. A*, 2018, **6**, 19775-19781.
24. N. Wang, G. Cheng, L. Guo, B. Tan and S. Jin, *Adv. Funct. Mater.*, 2019, **29**, 1904781.
25. X. Wang, L. Chen, S. Y. Chong, M. A. Little, Y. Wu, W.-H. Zhu, R. Clowes, Y. Yan, M. A. Zwijnenburg, R. S. Sprick and A. I. Cooper, *Nat. Chem.*, 2018, **10**, 1180-1189.
26. L. Stegbauer, K. Schwinghammer and B. V. Lotsch, *Chem. Sci.*, 2014, **5**, 2789-2793.
27. L. Li, W. Fang, P. Zhang, J. Bi, Y. He, J. Wang and W. Su, *J. Mater. Chem. A*, 2016, **4**, 12402-12406.
28. C. Mo, M. Yang, F. Sun, J. Jian, L. Zhong, Z. Fang, J. Feng and D. Yu, *Adv. Sci.*, 2020, **7**, 1902988.
29. J. Xu, C. Yang, S. Bi, W. Wang, Y. He, D. Wu, Q. Liang, X. Wang and F. Zhang, *Angew. Chem. Int. Ed.*, 2020, **59**, 23845.
30. K. Wang, Z. Jia, Y. Bai, X. Wang, S. E. Hodgkiss, L. Chen, S. Y. Chong, X. Wang, H. Yang, Y. Xu, F. Feng, J. W. Ward and A. I. Cooper, *J. Am. Chem. Soc.*, 2020, **142**, 11131-11138.
31. A. F. M. El-Mahdy, A. M. Elewa, S.-W. Huang, H.-H. Chou and S.-W. Kuo, *Adv. Opt. Mater.*, 2020, **n/a**, 2000641.
32. M.-Y. Gao, C.-C. Li, H.-L. Tang, X.-J. Sun, H. Dong and F.-M. Zhang, *J. Mater. Chem. A*, 2019, **7**, 20193-20200.
33. L. Guo, Y. Niu, S. Razzaque, B. Tan and S. Jin, *ACS Catal.*, 2019, **9**, 9438-9445.
34. M. Luo, Q. Yang, K. Liu, H. Cao and H. Yan, *Chem. Commun.*, 2019, **55**, 5829-5832.
35. S.-Y. Ding, P.-L. Wang, G.-L. Yin, X. Zhang and G. Lu, *Int. J. Hydrogen Energ.*, 2019, **44**, 11872-11876.
36. D. Wang, H. Zeng, X. Xiong, M.-F. Wu, M. Xia, M. Xie, J.-P. Zou and S.-L. Luo, *Sci. Bull.*, 2019, 10.015.
37. D. Wang, X. Li, L.-L. Zheng, L.-M. Qin, S. Li, P. Ye, Y. Li and J.-P. Zou, *Nanoscale*, 2018, **10**, 19509-19516.
38. Y.-J. Cheng, R. Wang, S. Wang, X.-J. Xi, L.-F. Ma and S.-Q. Zang, *Chem. Commun.*, 2018, **54**, 13563-13566.
39. H. Wang, C. Qian, J. Liu, Y. Zeng, D. Wang, W. Zhou, L. Gu, H. Wu, G. Liu and Y. Zhao, *J. Am. Chem. Soc.*, 2020, **142**, 4862-4871.
40. Y. Wang, W. Hao, H. Liu, R. Chen, Q. Pan, Z. Li and Y. Zhao, *Nat. Commun.*, 2022, **13**, 100.
41. W. Li, X. Ding, B. Yu, H. Wang, Z. Gao, X. Wang, X. Liu, K. Wang, J. Jiang, *Adv. Funct. Mater.*, 2022, **32**, 2207394.
42. H. Yan, Y.-H. Liu, Y. Yang, H.-Y. Zhang, X.-R. Liu, J.-Z. Wei, L.-L. Bai, Y. Wang, F.-M. Zhang, *Chem. Eur. J.*, **431**, 133404.
43. S. Ma, T. Deng, Z. Li, Z. Zhang, J. Jia, Q. Li, G. Wu, H. Xia, S.-W. Yang, X. Liu, *Angew. Chem. Int. Ed.*, 2022, **61**, e202208919.